

# Optical spectral reflectance of human articular cartilage - relationships with tissue structure, composition and mechanical properties

Jussi Kinnunen,<sup>1,\*</sup> Simo Saarakkala,<sup>2</sup> Markku Hauta-Kasari,<sup>3</sup>  
Pasi Vahimaa,<sup>1</sup> and Jukka S. Jurvelin<sup>4</sup>

<sup>1</sup>University of Eastern Finland, Department of Physics and Mathematics, P.O.B. 111, FI-80101, JOENSUU, Finland

<sup>2</sup>University of Oulu and Oulu University Hospital, Department of Diagnostic Radiology, P.O.B. 5000, FI-90014, OULU, Finland

<sup>3</sup>University of Eastern Finland, School of Computing, P.O.B. 111, FI-80101, JOENSUU, Finland

<sup>4</sup>University of Eastern Finland, Department of Applied Physics, P.O.B. 1627, FI-70211, KUOPIO, Finland

[\\*jussi.kinnunen@uef.fi](mailto:jussi.kinnunen@uef.fi)

**Abstract:** The information from spectral reflectance of articular cartilage has been related to the integrity of the tissue. This study explores more in detail the interrelations between the cartilage composition, structure and mechanical properties, and optical spectral reflectance. Using human osteochondral samples the reflectance spectral images of articular cartilage were captured and analyzed by using CIELAB color space as well as principal component analysis. With both analysis methods statistically significant correlations were observed between the reflectance and histological integrity, as assessed by Mankin scoring, tissue proteoglycan content and dynamic modulus. In thick human cartilage, the reflectance was found to be independent of the cartilage thickness, suggesting negligible influence of the underlying subchondral bone. Based on the present results diagnostically relevant information on cartilage quality can be extracted using optical spectral reflectance measurements. These measurements could be feasible during arthroscopic surgery when more in-depth information of the properties of articular cartilage is needed.

© 2011 Optical Society of America

**OCIS codes:** (300.6550) Spectroscopy, visible; (330.1730) Colorimetry; (170.3880) Medical and biological imaging.

---

## References and links

1. M. M. C. Steenvoorden, T. W. J. Huizinga, N. Verzijl, R. A. Bank, H. K. Ronda, H. A. F. Luning, F. P. J. G. Lafeber, R. E. M. Toes, and J. DeGroot, "Activation of receptor for advanced glycation end products in osteoarthritis leads to increased stimulation of chondrocytes and synoviocytes," *Arthritis Rheum.* **54**, 253–263 (2006).
2. V. M. Monnier, R. R. Kohn, and A. Cerami, "Accelerated age-related browning of human collagen in diabetes mellitus," *Proc. Natl. Acad. Sci. U.S.A.* **81**, 583–587 (1984).
3. G. Wyszecki and W. S. Stiles, *Color Science* 2nd ed. (Wiley, 2000).

4. K. Hattori, K. Uematsu, Y. Tanikake, T. Habata, Y. Tanaka, H. Yajima, and Y. Takakura, "Spectrocolorimetric assessment of cartilage plugs after autologous osteochondral grafting: correlations between color indices and histological findings in a rabbit model," *Arthritis Res. Ther.* **9**, R88 (2007).
5. K. Hattori, K. Uematsu, H. Matsumori, Y. Dohi, Y. Takakura, and H. Ohgushi, "Spectrocolorimetric evaluation of repaired articular cartilage after a microfracture," *BMC Res. Notes* **1**, 87 (2008).
6. Y. Ishimoto, K. Hattori, H. Ohgushi, K. Uematsu, Y. Tanikake, Y. Tanaka, and Y. Takakura, "Spectrocolorimetric evaluation of human articular cartilage," *Osteoarthritis Cartilage* **17**, 1204–1208 (2009).
7. J. Kinnunen, J. S. Jurvelin, J. Mäkitalo, M. Hauta-Kasari, P. Vahimaa, and S. Saarakkala, "Optical spectral imaging of degeneration of articular cartilage," *J. Biomed. Opt.* **15**, 046024 (2010).
8. P. Å. Öberg, T. Sundqvist, and A. Johansson, "Assessment of cartilage thickness utilising reflectance spectroscopy," *Med. Biol. Eng. Comput.* **42**, 3–8 (2004).
9. C. Qu, J. Rieppo, M. M. Hyttinen, M. J. Lammi, I. Kiviranta, J. Kurkijärvi, J. S. Jurvelin, and J. Töyräs, "Human articular cartilage proteoglycans are not undersulfated in osteoarthritis," *Connect. Tissue Res.* **48**, 27–33 (2007).
10. J. Kurkijärvi, M. Nissi, I. Kiviranta, J. Jurvelin, and M. Nieminen, "Delayed gadolinium-enhanced MRI of cartilage (dGEMRIC) and  $T_2$  characteristics of human knee articular cartilage: Topographical variation and relationships to mechanical properties," *Magn. Reson. Med.* **52**, 41–46 (2004).
11. H. Nieminen, P. Julkunen, J. Töyräs, and J. Jurvelin, "Ultrasound speed in articular cartilage under mechanical compression," *Ultrasound Med. Biol.* **33**, 1755–1766 (2007).
12. M. Nieminen, "Prediction of biomechanical properties of articular cartilage with quantitative magnetic resonance imaging," *J. Biomech.* **37**, 321–328 (2004).
13. P. Kiviranta, J. Töyräs, M. T. Nieminen, M. S. Laasanen, S. Saarakkala, H. J. Nieminen, M. J. Nissi, and J. S. Jurvelin, "Comparison of novel clinically applicable methodology for sensitive diagnostics of cartilage degeneration," *Eur. Cells Mater.* **13**, 46–55 (2007).
14. H. J. Mankin, H. Dorfman, L. Lippiello, and A. Zarins, "Biochemical and metabolic abnormalities in articular cartilage from osteo-arthritic human hips. II. correlation of morphology with biochemical and metabolic data," *J. Bone Jt. Surg., Am. Vol.* **53**, 523–537 (1971).
15. B. Mandelbaum and D. Waddell, "Etiology and pathophysiology of osteoarthritis," *Orthopedics* **28**, s207–214 (2005).
16. M. S. Laasanen, J. Töyräs, R. K. Korhonen, J. Rieppo, S. Saarakkala, M. T. Nieminen, J. Hirvonen, and J. S. Jurvelin, "Biomechanical properties of knee articular cartilage," *Biorheology* **40**, 133–140 (2003).
17. D. W. Ebert, "Articular cartilage optical properties in the spectral range 300–850 nm," *J. Biomed. Opt.* **3**, 326–333 (1998).
18. J. Rieppo, J. Töyräs, M. T. Nieminen, V. Kovanen, M. M. Hyttinen, R. K. Korhonen, J. S. Jurvelin, and H. J. Helminen, "Structure-function relationships in enzymatically modified articular cartilage," *Cells Tissues Organs* **175**, 121–132 (2003).
19. H. Nieminen, Y. Zheng, S. Saarakkala, Q. Wang, J. Töyräs, Y. Huang, and J. Jurvelin, "Quantitative assessment of articular cartilage using high-frequency ultrasound: research findings and diagnostic prospects," *Crit. Rev. Biomed. Eng.* **37**, 461–494 (2009).
20. J. Qu, C. MacAulay, S. Lam, and B. Palcic, "Optical properties of normal and carcinomatous bronchial tissue," *Appl. Opt.* **33**, 7397–7405 (1994).
21. R. K. Korhonen, M. S. Laasanen, J. Töyräs, R. Lappalainen, H. J. Helminen, and J. S. Jurvelin, "Fibril reinforced poroelastic model predicts specifically mechanical behavior of normal, proteoglycan depleted and collagen degraded articular cartilage," *J. Biomech.* **36**, 1373–1379 (2003).
22. M. Chandra, K. Vishwanath, G. D. Fichter, E. Liao, S. J. Hollister, and M. Mycek, "Quantitative molecular sensing in biological tissues: an approach to non-invasive optical characterization," *Opt. Express* **14**, 6157–6171 (2006).

---

## 1. Introduction

Degeneration of the articular cartilage, typical to osteoarthritis (OA) or rheumatoid arthritis (RA), is known to produce visual changes, i.e., the loss of glisten, change in tissue color and fibrillation of the cartilage surface. Color of the cartilage can turn from white into more yellowish or even brown [1]. The browning of cartilage is believed to be related to the advanced glycation end products (AGE) [2], and it is age-related. Several diseases, such as diabetes mellitus, can also accelerate the browning of the cartilage [2]. During arthroscopic examination, degenerative color changes of the articular cartilage are visually assessed. Obviously, this kind of assessment is subjective and the outcome depends on the evaluator. The color can also be assessed by using a conventional RGB camera. Both visual observation and RGB camera inspection are limited by the number of detector spectral sensitivities. This can be overcome by

using spectral based methods. The use of spectral camera reduces the possibility to observe the same RGB output for several different color signals, i.e., metamerism [3]. However, the extraction of relevant information from the measured spectral reflectance can be challenging. In articular cartilage research, the spectral data is often projected into some lower dimensional space or coordinate system such as CIELAB 1976 [4–6]. We have earlier shown that principal component analysis (PCA) can be used for spectral projection, and to effectively extract information that is related to the integrity of bovine articular cartilage [7]. It has also been speculated that the measured optical reflectance is affected by the reflectance of subchondral bone [4, 6, 8], being stronger in thin cartilage. In the present study, we used optical spectral reflectance measurements to characterize normal and osteoarthritic human articular cartilage. Specifically, we related the optical results with the tissue integrity, as quantified by the histological [9], biochemical [9] and biomechanical [10, 11] reference measurements.

## 2. Materials and methods

### 2.1. Articular cartilage samples

The samples for optical measurements were collected in our earlier studies [9–11]. Briefly, cylindrical osteochondral specimens with full thickness articular cartilage (diameter = 16 mm) were harvested from human cadaver knees ( $n = 13$ , age 25–77 years) in Jyväskylä Central Hospital, Jyväskylä, Finland (permission 1781/32/200/01, National Authority of Medicolegal Affairs, Helsinki, Finland). The samples originated from five anatomical locations; lateral femoral condyle (FLC), medial femoral condyle (FMC), medial tibial plateau (TMP), lateral tibial plateau (TLP) and femoral groove (FG) (total  $n = 65$ ). Cylindrical disks were cut into several pieces for the use in further analyses, immersed in phosphate buffered saline (PBS; Euroclone Ltd., Paignton Devon, UK) containing enzyme inhibitors 5 mM ethylenediaminetetraacetic acid (EDTA; Merck, Darmstadt, Germany) and 5 mM benzamidine HCl (Sigma, St. Louis, MO) and stored in a freezer. Use of the frozen samples is a common practice in cartilage research. After thawing the optical measurements were conducted to a sample, cut as a sector (1/4 or 1/2) from the original cylindrical disk.

### 2.2. Optical measurements and analysis

The methods for acquiring of spectral images and image analysis have been described in detail in our earlier study on bovine articular cartilage [7]. The spectral images were collected in the wavelength range of 420–720 nm with 7 nm sampling steps in standard 45/0 geometry (45 deg illumination and normal imaging angle) using a Nuance liquid crystal tunable filter (LCTF) spectral camera (model N-MSI-420-10, Cambridge Research & Instrumentation, Woburn, Massachusetts) (Fig. 1).

The samples, immersed in PBS during measurements, were illuminated by halogen light and measured through the glass window of a custom-made sample container. The reflectance of the samples was calculated as a ratio of the measured spectral data of reflected light from the sample and the white reference material (ODM98, Gigahertz-Optik GmbH, Germany). The position of front surface of the reference and cartilage samples was constant, i.e., at the same distance and angle to the light source and the detector. The pixel resolution of the images was 60.7 pixels/mm and spatial resolution 14.25 lp/mm. The original image size was 14 x 14 mm. The reflectance information was projected into XYZ color space using D65 standard daylight and CIE 1931 standard observer. These XYZ values indicate the tristimulus values of the object color for an observer with the cone spectral sensitivities corresponding to those of CIE 1931 standard observer. The D65 daylight represents the spectral power distribution of the daylight with a correlated color temperature of 6500 K. Eventually, the non-linear transform of XYZ to CIELAB coordinate system was performed [3] in order to compare the results with those of the

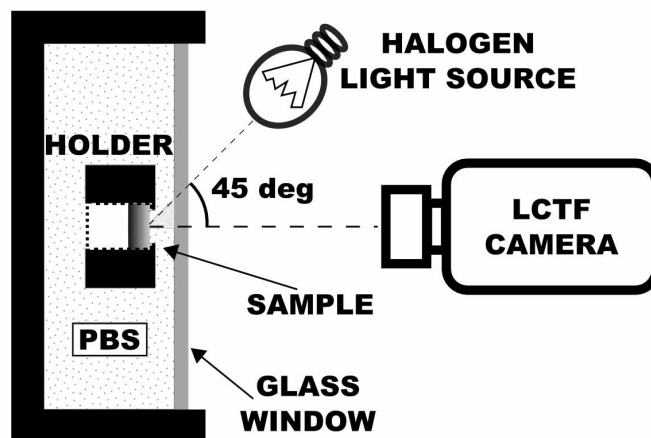


Fig. 1. The measurement setup as viewed from top. The sample was placed in a holder in the container which was completely filled with phosphate buffered saline (PBS). The sample was illuminated and detected through a glass window.

other authors [4–6]. The CIELAB system includes three coordinates;  $L^*$  for the lightness of the color (from 0 = black to 100 = white),  $a^*$  for redness/greenness ( $a^* < 0$  is greenish and  $a^* > 0$  is reddish) and  $b^*$  for blueness/yellowness ( $b^* < 0$  is bluish and  $b^* > 0$  is yellowish).

Moreover, the PCA base vectors were calculated for multiple subsets of the reflectance spectra as described in [7]. PCA generates for a given data set orthonormal base vectors which are optimized for reproduction of the variation of the original data. The PCA was done separately for the spectra measured at different anatomical locations and the PCA base vectors obtained were combined to the set of PCA base vectors generated earlier [7]. The suitable base vectors (Base 1, 2 and 3 vector) were chosen based on the finding how their projections represent cartilage reference properties. The projection can be realized, e.g., with optical filters that modify sensor spectral sensitivity to match with the shape of a base vector. If the base vector has both positive and negative values, two filters can be used. The obtained spectral image data, presenting the reflectance of the sample, was averaged at the center of each sample (200 x 200 pixels approx. 3.3 x 3.3 mm). The data analysis was done with MATLAB (v. 7.9.0, MathWorks Inc., Natick, Massachusetts).

### 2.3. Reference measurements

All reference biomechanical, histological and biochemical measurements, using adjacent tissues from the same cylindrical disks (diameter = 16 mm), were conducted and reported in our earlier studies [9–11]. The dynamic modulus  $E_{dyn}$  for the studied samples [10] was determined by using unconfined compression test (1 Hz sinusoidal loading and 1% strain amplitude) as described by Nieminen et al. [12]. The dynamic modulus indicates the compressive stiffness of articular cartilage under physiologically relevant loading rates. The modulus is significantly correlated with the integrity of tissue collagen network, and is secondarily contributed by the swelling pressure induced by proteoglycans. In early cartilage degeneration, the modulus goes down as the collagen network is disrupted [13].

The uronic acid (UA) content (normalized by the wet weight) for the samples, i.e., a measure of the tissue proteoglycan content, was determined in [9]. To determine proteoglycan concentration of the samples, uronic acid content was quantified from glycosaminoglycans extracted from the samples and normalized to the wet weight of the tissue. Reduction of cartilage proteo-

glycan content takes place in cartilage degeneration. In principle, the higher the proteoglycan content is, the better quality and biomechanical properties cartilage shows.

Further, the histological tissue integrity was evaluated using the Mankin scoring of the histological sections [14]. Mankin scoring is a traditional microscopic technique to quantitate histological structure of cartilage. It includes assessment several tissue features, such as surface irregularities and clefts, cellularity, proteoglycan content by safranin O staining and tidemark integrity [14]. The higher the Mankin score is, the lower is the structural integrity (quality) of tissue. The samples were divided into three groups [9]; normal (score = 0-1,  $n = 16$ ), early OA (score = 2-3,  $n = 34$ ) and advanced OA (score = 4-9,  $n = 15$ ). Thickness of the cartilage at each sample was assessed by Nieminen et al. [11].

#### 2.4. Statistical analysis

The Pearson's correlation test was used to evaluate the linear association between the optical parameters and the reference parameters. However, because of the ranked nature of the Mankin scoring, the Spearman's correlation analysis was used when relating histological Mankin score with the optical parameters.

### 3. Results

The mean spectra of the samples in three groups with normal, early OA and advanced OA cartilage (Mankin score 0-1, 2-3 and  $>3$  respectively) had similar shape, but the total reflectance was decreased in advanced OA group compared to normal or early OA groups (Fig. 2). It is noteworthy that the variation between spectra inside each group was large compared to the differences between mean spectra (Fig. 2).

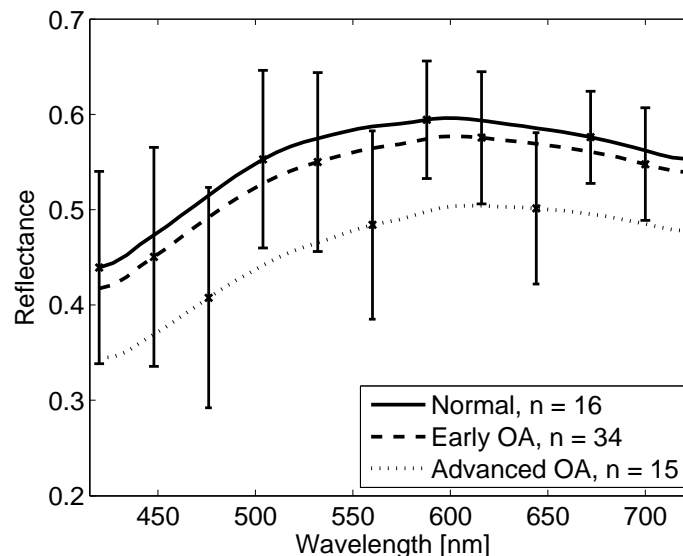


Fig. 2. The mean reflectance spectra for normal (Mankin score = 0-1) cartilage, cartilage with early OA (Mankin score = 2-3), and advanced OA (Mankin score = 4-9). The wavelength dependent standard deviation for normal, early OA and advanced OA spectra varied between 0.045-0.111, 0.058-0.115 and 0.067-0.112 respectively.

The  $L^*$ -coordinate, indicating the sample lightness [3], showed a significant negative correlation with the tissue Mankin score ( $r = -0.354$ ,  $n = 65$ ,  $p < 0.01$ ), whereas the  $a^*$ - and the

$b^*$ -coordinates were not significantly related to Mankin score (Table 1, Fig. 3). Further, projections to Base 2 vector correlated with the Mankin score (Table 1, Fig. 4). All optical parameters were significantly related to the uronic acid content of samples (Table 1). Projection to Base 1 vector (Table 1, Fig. 4) correlated significantly with the dynamic modulus ( $r = 0.510$ ,  $n = 65$ ,  $p < 0.001$ ). The  $L^*$ -coordinate and projection to Base 2 vector showed weaker associations with the dynamic modulus (Table 1). No optical parameter was significantly correlated with the cartilage thickness (Table 1).

Table 1. Linear Correlation Coefficients Between the Optical Parameters and Mankin Score, Uronic Acid (UA) Content ( $[\mu\text{g}/\text{mg}]$  Wet Weight), Dynamic Modulus and Thickness of the Human Articular Cartilage Samples ( $n = 65$ ). The Spearman's correlation analysis was used with Mankin score.

	$L^*$	$a^*$	$b^*$	Base 1	Base 2	Base 3
Mankin score	-0.354 *	0.239	0.178	-0.195	-0.349 *	-0.231
UA content	0.482 **	-0.580 **	-0.373*	0.375*	0.455**	0.667 **
dynamic modulus	0.375 *	-0.265	-0.058	0.510 **	0.364 *	0.292
thickness	-0.070	-0.147	-0.032	0.052	-0.077	0.210

\* $p < 0.01$ , \*\* $p < 0.001$ .

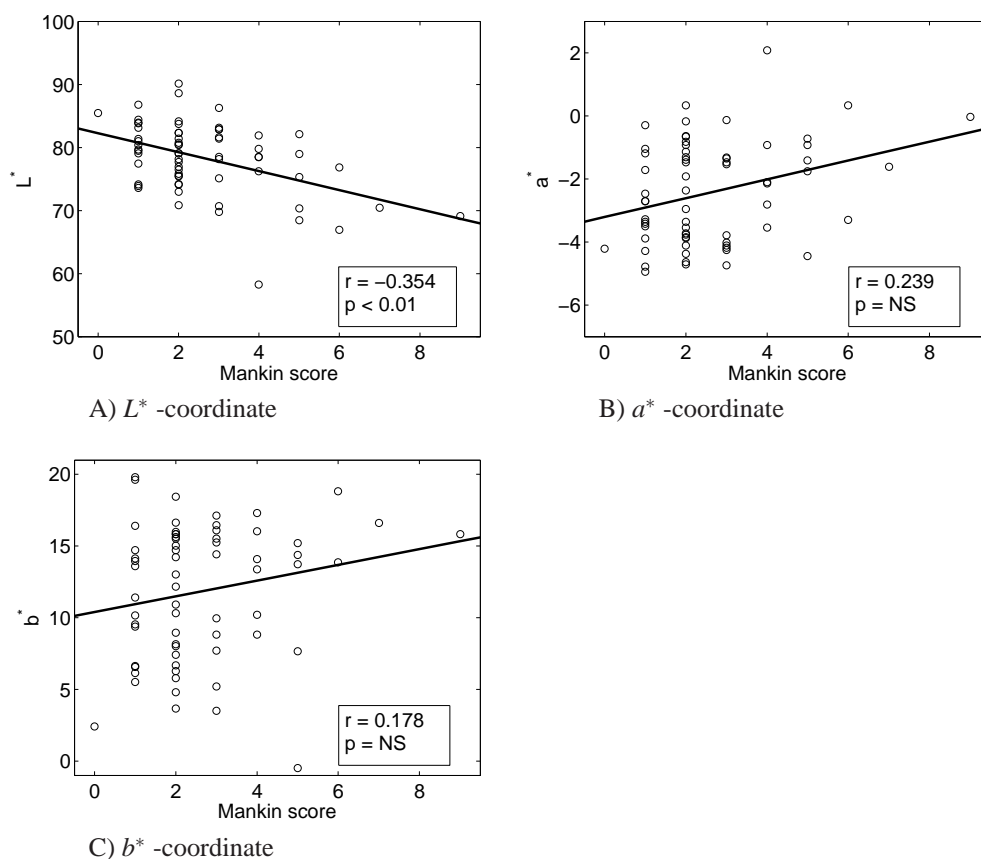


Fig. 3. The CIELAB color coordinates as a function of the Mankin score ( $n = 65$ ).

The spectral images of samples with different Mankin score and uronic acid content were projected to Base 2 and Base 3 vectors, respectively (Fig. 4, 5). The projection images also showed the decrease in the projection when the Mankin score increased and increase in the projection when the uronic acid content increased (Fig. 5).

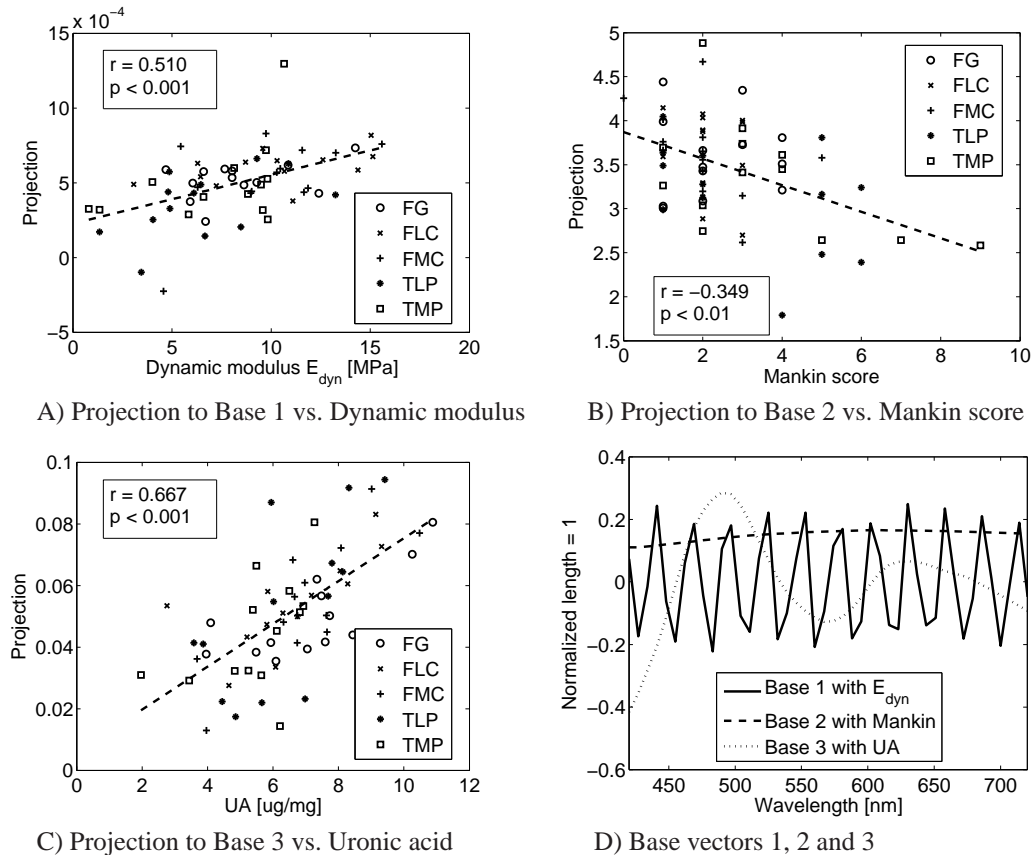


Fig. 4. The scatter plots for spectral projections as a function of dynamic modulus (A), Mankin score (B) and uronic acid (C), as well as used base vectors (D) for each of the projections. The legends FG, FLC, FMC, TLP and TMP denote the five anatomical locations; femoral groove, lateral femoral condyle, medial femoral condyle, lateral tibial plateau and medial tibial plateau, respectively. The base vectors (D) are all unit vectors.

#### 4. Discussion and conclusion

In the present study, we used optical spectral reflectance measurements for characterization of human articular cartilage and related the optical spectral reflectance results to tissue structure, composition, thickness and mechanical properties. The optical parameters were found to be significantly related to tissue integrity, as assessed by histological, biochemical and biomechanical analyses. In this study, the optical parameters (CIELAB coordinates and the projections of spectra to the used base vectors) could be considered as true material parameters as they were not related to thickness of articular cartilage. This highlights their potential for use as quantitative indices when diagnosing cartilage related disorders.

Under standardized conditions, the reflectance was found to decrease as cartilage degenera-

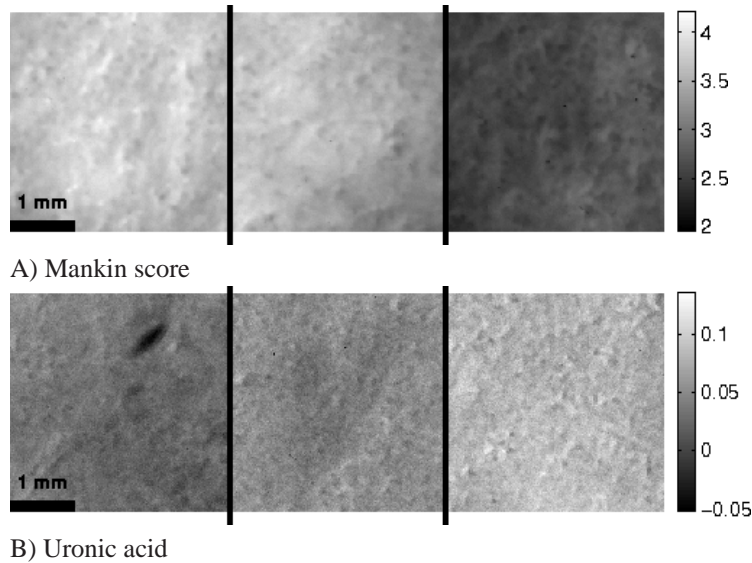


Fig. 5. Representative images for projections of samples with low (left), average (middle) and high (right) Mankin score (1, 3, 7, respectively) (upper panel) or uronic acid content (3.44, 6.32, 10.89 [ $\mu\text{g}/\text{mg}$ ], respectively) (lower panel). The trend in appearance from light to more dark along the increase in Mankin score, or from dark to more light along the increase in uronic acid content is evident.

tion advanced. We used the histological evaluation, i.e., Mankin scoring by three investigators from Safranin O stained blind coded sections, to evaluate microstructural integrity of articular cartilage. In OA, degradative processes exceed the ability of cartilage cells, chondrocytes, to maintain the extracellular matrix of articular cartilage [15], and arthritic cartilage is mechanically weak due to the disrupted collagen network and proteoglycan depletion. Mankin score evaluates several aspects related to characteristic OA changes, including superficial tissue changes such as surface fibrillation and depletion of proteoglycans. The optical parameters, especially  $L^*$  coordinate and projection to Base 2 vector, were significantly related to Mankin score and proteoglycan content assessed biochemically by uronic acid content [9]. The change in  $L^*$  is consistent with the results by Ishimoto et al. [6]. The  $a^*$  coordinate, while representing the redness/greenness, is often related to the blood and bone marrow of subchondral bone and cartilage opacity [4, 5]. In the present study, the proteoglycan content only correlated significantly with the coordinates  $a^*$  and  $b^*$ . As the  $a^*$  was negative and  $b^*$  positive in most samples (see Fig. 3(B) and 3(C)), the observed negative correlation indicates that cartilage with higher proteoglycan content is greener and less yellow.

The optical parameters in cartilage relate to structure and composition of the solid tissue matrix, and in degenerated tissue, disrupted collagen network, accompanied by the depletion of proteoglycans, alter light backscattering and produce the present changes in optical parameters recorded in the present study. Due to the same structural and compositional alterations, biomechanical properties of degenerated cartilage get inferior. In the present study, this was evidenced by the decrease of tissue dynamic modulus, known to be especially sensitive to integrity of collagen network [16]. Especially, projection to Base 1 vector was significantly correlated with the dynamic modulus. Thereby, the optical information was indicative to tissue structure, composition and also biomechanical properties.

In the present study with human cartilage we found no significant correlation between the



tissue thickness and reflectance, even when using PCA for extraction of optical features. Earlier, Öberg et al. showed a relationship between the thickness of bovine hip joint cartilage and light reflection from the tissue [8]. In their study, the thickness for the intact samples varied from 0.67 to 1.98 mm and the changes in thickness were conducted by grinding the cartilage, layer by layer. The exponential relation was found between the reflectance at 330 - 835 nm and the results from ultrasound thickness measurements. We have also observed similar thickness relation with the bovine knee cartilage with subchondral bone [7]. However, in the present study the human cartilage thickness was 1.38 - 3.64 mm, thus being mostly thicker than that in the study by Öberg et al. [8] and in our earlier study [7]. It is notable that in the study by Öberg et al., the exponential relation between the thickness and reflectance nearly saturated after thickness of 1 mm, suggesting that in thick cartilage, the effect of subchondral bone on optical reflection may be negligible. Ebert et al. [17] have estimated that the penetration depth of light at 350 – 850 nm varies between 0.6 - 3 mm on horse articular cartilage. In the present study, the variation in human cartilage thickness was of biological origin, not obtained by grinding. As native cartilage is non-homogeneous with highly layered collagen network structure [18], the original superficial, median and deep zones of cartilage were present in samples. After artificial thinning by grinding, not only the thickness but also the zonal structure of articular cartilage is modified. This makes more complex to evaluate objectively the effect of tissue thickness on optical measurements.

Our reference analysis, related to tissue structure, composition and mechanical properties, provided comprehensive information on cartilage integrity. However, they are not complete as no quantitative information on collagen content and architecture was available. Earlier, we have found that collagen network is an effective scatterer of both acoustic [19] and optical waves [17,20]. Further, biomechanical properties could be characterized more completely, e.g., by using fibril reinforced biphasic analyses where the model parameters specifically reflect the major components of the cartilage matrix, i.e., proteoglycans and collagen [21].

As a technical limitation, we could not analyze the same tissue but used adjacent samples for different optical, microscopic, biochemical and biomechanical methods. As the site-dependent variation of cartilage mechanical properties is well known [16], this will inevitably contribute to our results, and most probably lead to inferior structure-composition-biomechanical-optical property correlations. Pooling the data from different anatomical sites was considered justified, and data indicates no site-dependent clustering (Fig. 4). However, even with the above mentioned limitations our results are encouraging and imply that optical measurements may be feasible for cartilage diagnostics. Chandra et al. [22] used a fiber optic probe for detecting cartilage optical properties *in vitro*. In the present study, the changes in optical reflectance of human articular cartilage were significantly related to tissue composition, structure and properties. The CIELAB color coordinates can be easily calculated from the camera RGB values, and the projections to base vectors can be made by using a special light source with multiple exposures. Indeed, optical characterization of articular cartilage during arthroscopy may be a feasible procedure by modifying a regular video arthroscope. This could have significant clinical potential as arthroscopic evaluation of the joints is one of the most frequent surgical procedures in clinical medicine.

### **Acknowledgments**

The financial support from the Ministry of Education, Finland (University of Eastern Finland grant, projects 5741/Kuopio and 10102/Joensuu); and from the Academy of Finland (project 127198) is acknowledged. The assistance of Ms. Jaana Mäkitalo with the measurement of the cartilage samples is acknowledged.